interdisciplinary
ïoxicology

![sciendo logo] **sciendo**

ORIGINAL ARTICLE

Pixantrone, a new anticancer drug with the same old cardiac problems? An *in vitro* study with differentiated and non-differentiated H9c2 cells

Ana REIS-MENDES #, Marisa ALVES #, Félix CARVALHO, Fernando REMIÃO, Maria Lourdes BASTOS, Vera Marisa COSTA

UCIBIO-REQUIMTE, Laboratory of Toxicology, Faculty of Pharmacy, University of Porto, Porto, Portugal

 # Authors contributed equally to the work.

ABSTRACT

Pixantrone (PIX) is an anticancer drug approved for the treatment of multiple relapsed or refractory aggressive B-cell non-Hodgkin's lymphoma. It is an aza-anthracenedione synthesized to have the same anticancer activity as its predecessors, anthracyclines (*e.g.* doxorubicin) and anthracenediones (*e.g.* mitoxantrone), with lower cardiotoxicity. However, published data regarding its possible cardiotoxicity are scarce. Therefore, this work aimed to assess the potential cytotoxicity of PIX, at clinically relevant concentrations (0.1; 1; and 10 µM) in both non-differentiated and 7-day differentiated H9c2 cells. Cells were exposed to PIX for 48 h and cytotoxicity was evaluated through phase contrast microscopy, Hoescht staining and the 3-(4,5-dimethylthiazol-2-yl)-2,5-diphenyl tetrazolium bromide (MTT) reduction and neutral red (NR) uptake assays. Cytotoxicity was observed in differentiated and non-differentiated H9c2 cells, with detached cells and round cells evidenced by phase contrast microscopy, mainly at the highest concentration tested (10 µM). In the Hoechst staining, PIX 10 µM showed a marked decrease in the number of cells when compared to control but with no signs of nuclear condensation. Furthermore, significant concentration-dependent mitochondrial dysfunction was observed through the MTT reduction assay. The NR assay showed similar results to those obtained in the MTT reduction assay in both differentiated and non-differentiated H9c2 cells. The differentiation state of the cells was not crucial to PIX effects, although PIX toxicity was slightly higher in differentiated H9c2 cells. To the best of our knowledge, this was the first *in vitro* study performed with PIX in H9c2 cells and it discloses worrying cytotoxicity at clinically relevant concentrations.

KEY WORDS: Pixantrone; H9c2 cells; cardiotoxicity

ABBREVIATIONS:
DMEM: Dulbecco´s Modified Eagle medium; **DOX:** Doxorubicin; **EDTA:** Ethylenediamine tetraacetic acid; **EMA:** European Medicines Agency; **FBS:** Fetal bovine serum; **FDA:** Food and Drug Administration; **HBSS:** Hanks' balanced salt solution; **MTT:** 3-(4,5-dimethylth-iazol-2-yl)-2,5-diphenyl tetrazolium bromide; **MTX:** Mitoxantrone; **NHL:** Non-Hodgkin's lymphoma; **NR:** Neutral Red; **PBS:** Phosphate buffered saline; **PIX:** Pixantrone; **RA:** Retinoic acid; **ROS:** Reactive oxygen species

Introduction

Chemotherapy is still one of the most frequent strategies used against cancer. Anticancer drugs, however, lack total selectivity, which results in serious side effects (Hrynchak

Correspondence address:
Vera Marisa Costa
UCIBIO, REQUIMTE, Laboratory of Toxicology,
Faculty of Pharmacy, University of Porto
Rua de Jorge Viterbo Ferreira, 228,
4050-313 Porto, Portugal
TEL.: +315 22 0428596 • E-MAIL: veramcosta@ff.up.pt

et al., 2017; Reis-Mendes *et al.,* 2015). Cardiotoxicity is one of the most worrying side effect found in patients treated with anticancer drugs of several pharmacological groups, like anthracyclines [*e.g.* doxorubicin (DOX)] and anthracenediones [*e.g.* mitoxantrone (MTX)] (Hrynchak *et al.,* 2017; Reis-Mendes *et al.,* 2015). DOX has been used for almost 50 years, but cardiotoxicity has been a criti-cal and limiting side effect in its clinical use. MTX was synthesized with the purpose to maintain an effective anticancer potential yet without the cardiotoxicity, which characterized DOX (Conner, 1984). However, early data of

MTX demonstrated that cardiac toxicity was still a matter of concern (Stuart-Harris *et al.*, 1984). It was thus necessary to study the cardiotoxicity mechanisms of these compounds in order to find new ones that would be, in fact, less cardiotoxic. The mechanisms of cardiotoxicity of MTX are still poorly known, however several hypotheses have been suggested. The 5,8-dihydroxyphenyl ring of MTX was implicated in its cardiotoxicity through the formation of free radicals (Corbett *et al.*, 1981; El-Helw & Hancock, 2007). Additionally, MTX can form complexes with Fe^{3+} and lead to oxidative stress, although the Fe^{3+}-MTX complex is eight times less potent than Fe^{3+}-DOX in the production of the hydroxyl radical (Herman *et al.*, 1997; Malisza & Hasinoff, 1995). Actually, the oxidative stress hypothesis was the first considered as the culprit for MTX-induced cardiotoxicity, possibly because it has been linked to DOX-induced cardiotoxicity (Costa *et al.*, 2013). Therefore, the 5,8-dihydroxyphenyl ring of MTX was replaced by a pyridine ring to create an aza derivative. Moreover, the (ethylamino)-diethylamino side chains were substituted for (hydroxyethylamino)-ethylamino side chains, forming a powerful cytotoxic agent against *in vitro* and murine models of cancer, BBR 2778. This compound was later named pixantrone (PIX) (6,9-bis [(2-aminoethyl) amino] benzo[g]isoquinoline-5, 10-dione) (Krapcho *et al.*, 1994) (Figure 1).

PIX (Pixuvri®) was approved by the European Medicines Agency (EMA) in monotherapy in adult patients with relapsed or refractory aggressive B-cell non-Hodgkin's lymphoma (NHL) (EMA 2017; Péan *et al.*, 2013). PIX seems to have similar anticancer mechanisms when compared with MTX and anthracyclines, namely DOX (Volpetti *et al.*, 2014). Anthracyclines or anthracenediones kill tumor cells by intercalating in the DNA, inhibiting topoisomerase IIα, and forming double-strand breaks (Beggiolin *et al.*, 2001; Hasinoff *et al.*, 2016). These mechanisms are essentially due to the presence of the planar ring system that is composed by the four rings in anthracyclines and an amino-sugar, daunosamine, and the three rings in anthracenediones without any amino-sugar

(Beggiolin *et al.*, 2001; Hasinoff *et al.*, 2016). Moreover, the nitrogen atom in PIX was added in the anthracenedione chromophore to create an additional hydrogen bond, and in turn, modulate the DNA affinity and the interaction with topoisomerase II (El-Helw & Hancock, 2007). In fact, PIX works as a topoisomerase II inhibitor, as PIX induces formation of linear DNA in a cleavage assay with topoisomerase IIα and topoisomerase IIβ. In K562 cells, PIX also showed to cause DNA double-strand breaks (Hasinoff *et al.*, 2016).

While some efficacy has been demonstrated in relapsed aggressive NHL (Borchmann *et al.*, 2003; Pettengell *et al.*, 2012), the Food and Drug Administration USA (FDA) has not approved PIX use and it has only been conditionally approved in the EU for aggressive NHL (EMA, 2017). In fact, data regarding its cardiotoxicity are scarce, and lack of FDA approval is, in part, due to the inconsistencies shown by some of the studies carried out so far (FDA, 2010). In a Phase I clinical trial performed by Faivre *et al.* six patients with advanced solid tumors received a cumulative dose of 500 mg/m^2 (range, 560–1 460 mg/m^2) of PIX without any evidence of cardiotoxicity (Faivre *et al.*, 2001). Although not so widely used as its analogues, from the cardiac point of view, most authors consider PIX a safer drug than DOX or MTX. However, in a study by Dawson and collaborators, a patient treated with total dose of 1 120 mg/m^2, four cycles, showed signs of decreased left ventricular ejection (Dawson *et al.*, 2000) and a Phase III clinical trial using lower cumulative doses showed decreased ejection fraction in 19% of the patients treated with PIX (Pettengell *et al.*, 2012). As reported by the FDA, Phase II and Phase III clinical studies showed several inconsistences regarding PIX cardiotoxicity (FDA, 2010). There are also few *in vitro* studies aimed to evaluate the effects of PIX on cardiac cells (Hasinoff *et al.*, 2016), thus a better clarification concerning its possible cardiotoxicity is essential. Therefore, the main purpose of this work was to study PIX cardiotoxicity *in vitro* in non-differentiated and differentiated H9c2 cells as to elucidate its possible cardiotoxicity.
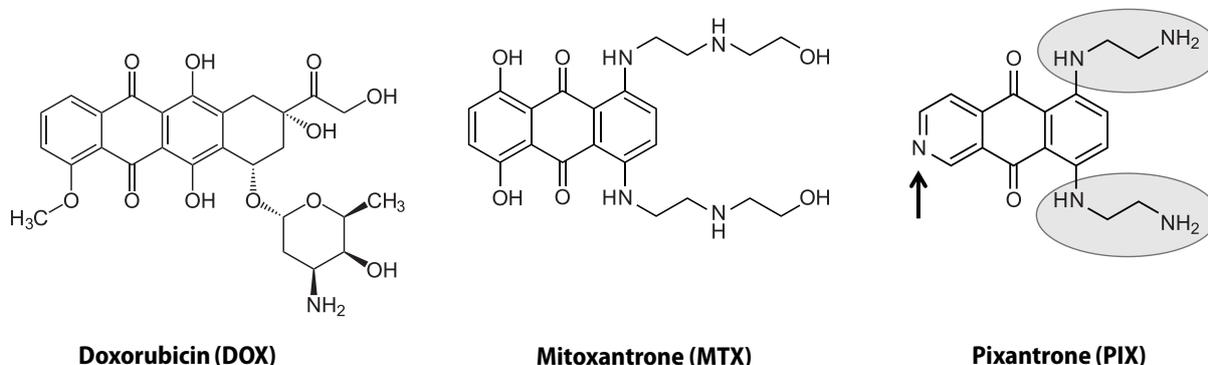
Figure 1. Chemical structure of DOX, MTX and PIX. DOX is composed by a tetracyclic quinone-hydroquinone chromophore, a carbonyl-containing side chain, and an aminosugar (daunosamine). MTX is a three-ring quinone-hydroquinone anthracenedione; its side chains lack carbonyl groups and MTX also lacks daunosamine. PIX differs from MTX in its lack of the hydroquinone, insertion of a nitrogen heteroatom in the same ring (black arrow), and substitution of (ethylamino)-diethylamino for (hydroxyethylamino)-ethylamino side chains (grey circles).

Materials and methods

Materials

Trypsin-EDTA solution, trypan blue solution 0.4% (w/v) and Dulbecco's Modified Eagle Medium (DMEM) high glucose, sodium dodecyl sulphate, hydrochloric acid, sodium bicarbonate, 3-(4,5-dimethylthiazol-2-yl)-2,5-diphenyl tetrazolium bromide (MTT), neutral red (NR) solution, Hoescht 33258 solution, dimethyl sulfoxide, retinoic acid (RA) and paraformaldehyde were obtained from Sigma-Aldrich (Germany). PIX was acquired from Abcam (United Kingdom). All sterile plastic material was obtained from Corning Costar (USA). Penicillin/streptomycin (10 000 units/mL/10 000 µg/mL) and the phosphate buffer solution (PBS) without calcium and magnesium were obtained from Biochrom (Germany). Fetal bovine serum (FBS), PBS with calcium and magnesium and Hank's saline solution (HBSS or "Hanks' balanced salt solution") were obtained from Gibco (United Kingdom).

Cell culture

Experiments were performed using H9c2 cells, a subclone of the original cell line derived from embryonic BD1X rat heart tissue (Kimes & Brandt, 1976). The rat cardiomyocyte derived H9c2 cell line was obtained from the European Collection of Cell Cultures [H9c2 cell line from rat (BDIX heart myoblast), Sigma-Aldrich (Germany)]. H9c2 cells have morphological similarities with immature embryonic cardiomyocytes, while preserving characteristics of adult cardiac cells (Hescheler *et al.,* 1991) and their metabolic characteristics are similar to those of the rat heart (Zordoky & El-Kadi, 2007). The cells are not fully differentiated in cardiomyocytes and remain in the proliferative state when 10% FBS is present in the culture medium (Rossato *et al.,* 2013). They are one of the most widely used *in vitro* model to study cardiotoxicity (Rossato *et al.,* 2013; Sardão *et al.,* 2009; Zordoky & El-Kadi, 2007). To obtain differentiated H9c2 cells, the cells are maintained in a low FBS (1%) medium enriched with 10 nM RA for 7 days (medium change every other day). This procedure enhances the cells' cardiac adult phenotype and decreases myogenic differentiation and cellular division (Menard *et al.,* 1999). Since PIX acts on cellular division, this later model can be seen as a good model to avoid the bias of high proliferation rates.

Experimental procedures in cell culture

Cell maintenance

While proliferating, cells were placed at 37 °C with 5% CO_2 in DMEM high glucose enriched by 10% of FBS, 100 units/ml penicillin and 100 µg/ml streptomycin. To prevent loss of myoblast cells, cell cultures were subcultured through trypsinization before reaching 70–80% confluence and were used before passage 29 (Reis-Mendes *et al.,* 2017; Ruiz *et al.,* 2012).

H9c2 were used in two differentiation states: non-differentiated and differentiated. The trypsinization step was performed prior to each seeding and to maintain cells in culture. Non-differentiated H9c2 cells were seeded at a density of 8 750 cells/cm^2 (Sardão *et al.,* 2009). Twenty-four hours after seeding, the cells were incubated with different PIX concentrations (0.1, 1 and 10 µM) for 48 h. The concentrations were chosen based on the plasma values of PIX found in a Phase I clinical trial (Faivre *et al.,* 2001). Maximum concentration (Cmax) of PIX 1 h after intravenous doses (37.5 to 150 mg/m^2) ranged between 1–7 µM (Faivre *et al.,* 2001).

H9c2 cells were also differentiated with DMEM supplemented with 1% FBS, RA 10 nM and antibiotics, with medium change every other day for 7 days, after being seeded in a density of 6 000 cells/cm^2 (Reis-Mendes *et al.,* 2017). After the 7-day differentiation, cells were incubated with PIX (0.1, 1 or 10 µM) for 48 h.

Stock solutions of PIX were prepared in sterile PBS and PBS was used as control. PIX solutions were made monthly and frozen at −20 °C to guarantee stability.

Phase contrast microscopy

Phase-contrast microscopy morphological evaluation was performed to determine the effects of PIX after a 48-h incubation in both non-differentiated and differentiated cells. A Nikon Eclipse TS100 equipped with a Nikon DS-Fi1 camera (Japan) was used.

Hoescht staining

To evaluate the effects of PIX on the nuclear morphology of both non-differentiated and differentiated H9c2 cells, Hoechst staining was performed, as previously described (Reis-Mendes *et al.,* 2017). Cells were examined in a Nikon Eclipse TS100 equipped with a Nikon DS-Fi1 camera (Japan) using a fluorescent filter (λexcitation = 346 nm and λemission = 460 nm).

Cytotoxicity evaluation

For the evaluation of PIX putative cytotoxicity, two assays were used: the NR lysosomal uptake and the MTT reduction assays. Both methods were performed 48 h after the cells' exposure to PIX and the assays are described as follows.

MTT reduction assay

The MTT colorimetric assay is based on the reduction of the tetrazolium salt with formazan formation and it was performed as previously described (Reis-Mendes *et al.,* 2017; Rossato *et al.,* 2013). The spectrophotometric measurement of the formazans was done at 550 nm in a multi-well plate reader (PowerWaveXS, BioTek Instruments Inc., USA).

Neutral red lysosomal uptake assay

The NR dye enters the viable cells and concentrates in lysosomes. The NR uptake assay was performed as previously described (Reis-Mendes *et al.,* 2017). The absorbance was read at 540 and 690 nm (reference) on a multi-well plate reader (Biotech Synergy HT, USA).

Statistical analysis

The results are expressed as mean ± standard deviation. Outliers were evaluated by the ROUT test. The D'Agostino & Pearson normality test was used to evaluate data distribution. A parametric analysis of variance (ANOVA) was performed when data distribution was normal, followed by the Tukey's *post-hoc* test. When data did not follow a normal distribution, statistical analysis was performed using the Kruskal-Wallis test, followed by the Dunn's *post-hoc* test when a significant *p*-value was reached. Statistical significance was reached when *p*<0.05. All statistical analyses were performed in GraphPad Prism 7 software (USA). All details of the statistical analyses can be found in the figure legends.

Results

Morphological evaluation of pixantrone-exposed non-differentiated H9c2 cells showed cytotoxicity at the highest concentration tested with no signs of condensed nuclei

Cells were morphologically assessed through phase-contrast microscopy after a 48-h exposure to PIX. H9c2 cells were incubated with PIX (0.1, 1 and 10 μM), as described in the Methods section. Control cells had mostly cells with polygonal form attached to the bottom of the wells with very few detached cells (Figure 2A). At 48 h, PIX 0.1 and 1 μM had no signs of cellular damage (Figures 2B and 2C), while PIX 10 μM caused a clear cytoplasmic injury in non-differentiated H9c2 cells and most cells were round and detached (Figure 2D). Hoechst staining was used to evaluate the nuclear morphology after the 48-h incubation. A slight decrease in the number of cells in PIX 0.1 μM (Figure 2F) and PIX 1 μM (Figure 2G) exposed cells was observed when compared to the control wells (Figure 2E), with some nuclear fragmentation in non-differentiated H9c2 cells incubated with PIX

0.1 μM (Figure 2F). PIX 10 μM caused a marked decrease in the number of cells, with very few fluorescent nuclei in the field (Figure 2H).

Pixantrone caused significant cytotoxicity in non-differentiated H9c2 cells according to the neutral red and MTT assays

The NR uptake and the MTT reduction assays were done after the 48-h incubation in non-differentiated H9c2 cells (Figure 3). In the NR assay, PIX caused a concentration dependent decrease in the uptake of the vital dye: 0.1 μM presented values 87.07±6.07%, 1 μM of 76.25±8.21% and 10 μM of 23.08±13.53% (Figure 3A). In the MTT assay, PIX produced a significant mitochondrial dysfunction at 0.1 μM (89.32±7.49%), 1 μM (84.06±8.82%) and 10 μM (47.00±7.39%) concentrations when compared to control cells (100.0±3.51%) (Figure 3B).

Pixantrone caused higher cellular damage in differentiated than in non-differentiated H9c2 cells

The differentiation with 10 nM RA and 1% FBS for 7 days led to morphological changes, making H9c2 cells more resembled to the cardiac phenotype. The differentiation protocol dramatically reduced cell division, and the cell bodies became smaller and fusiform. Overall, differentiated control cells showed a more organized network, bearing a cardiac-like morphology, as shown by phase-contrast morphology (Figure 4A). In differentiated H9c2 cells at 48 h, PIX incubation caused cell injury with cytoplasmic injury observed at PIX 1 μM and PIX 10 μM. In the latter concentration, the cellular damage was substantial (Figure 4D). In the Hoechst staining, a slight decrease in the number of cells for PIX 0.1 μM (Figure 4F) and PIX 1 μM (Figure 4G) was observed when compared to the control wells (Figure 4E). PIX 10 μM was able to cause a marked decrease in the number of cells, with very few fluorescent nuclei observed in the field (Figure 4H).
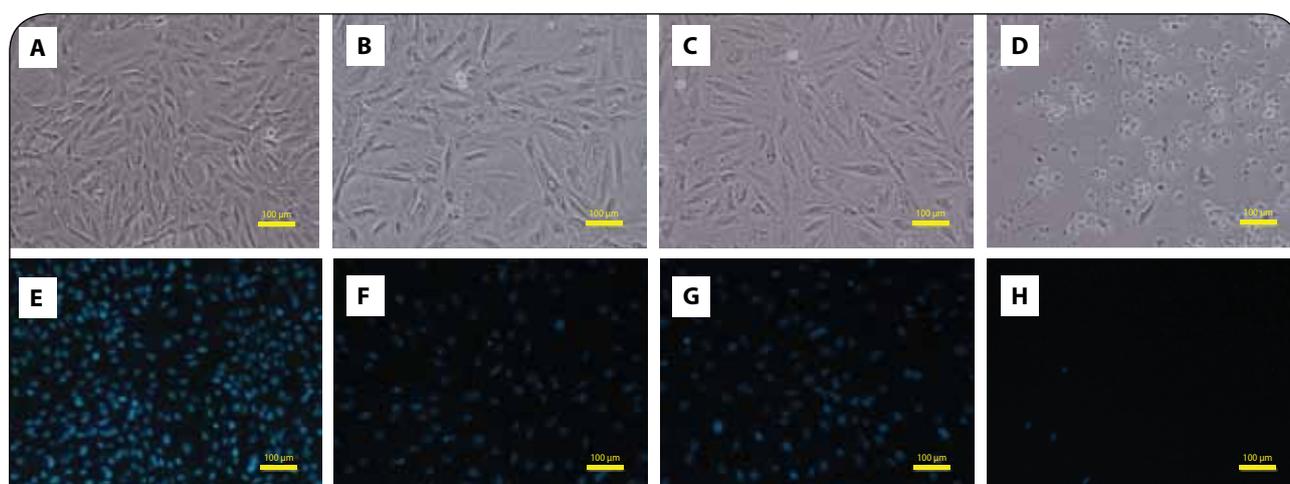
Figure 2. PIX causes cytotoxicity in non-differentiated H9c2 without signs of condensed nuclei. Phase contrast microscopy (A, B, C, D) and fluorescence microscopy (Hoechst 33258 staining) (E, F, G, H) images of non-differentiated H9c2 cells after a 48-h exposure to PBS (A and E), 0.1 μM PIX (B and F), 1 μM PIX (C and G) or 10 μM PIX (D and H). Images are representative of two independent experiments (scale bar 100 μm).

Pixantrone caused a concentration-dependent mitochondrial and lysosome dysfunction in differentiated H9c2 cells

In the NR assay performed in differentiated H9c2 cells, the highest concentration of PIX (10 μM) caused a substantial impairment of lysosomal uptake of the vital dye (7.44±3.83%) when compared to control cells (100.0±2.03%). NR uptake in PIX 0.1 μM was 93.51±3.22% and in PIX 1 μM, it was 86.15±3.06% (Figure 5A). In the MTT reduction assay, PIX 10 μM (39.54±2.40%) caused a significant mitochondrial dysfunction when compared to control cells (100.0±2.90%) (Figure 5B). The highest concentration of PIX (10 μM) caused a significant higher cytotoxicity when compared to PIX 1 μM or PIX 0.1 μM (89.42±6.29% and 91.59±5.27%, respectively).

Discussion

The present study is the first report on the toxicity of pharmacologically relevant concentrations of PIX (0.1; 1 and 10 μM) in H9c2 cells. PIX was cytotoxic at all concentrations tested, as evaluated by phase contrast microscopy, MTT reduction and NR uptake assays, in both differentiated and non-differentiated H9c2 cells.

A Phase III, multicentre, open-label, randomized trial was used to test the efficacy and safety of PIX in heavily pre-treated patients with relapsed or refractory aggressive NHL. The frequency of cardiac adverse events was higher in the PIX group than in the comparator group, where patients were treated with vinorelbine, oxaliplatin,
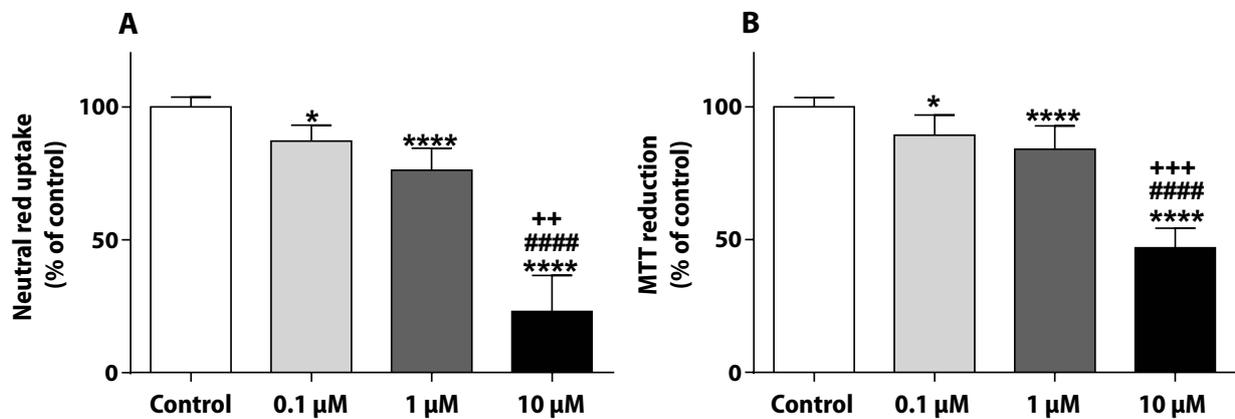
Figure 3. PIX leads to lysosomal and mitochondrial damage in non-differentiated H9c2. NR uptake (A) and MTT reduction (B) assays in non-differentiated H9c2 cells exposed to 0.1, 1 or 10 μM PIX for 48 h. Values are expressed as percentage of control and are shown as mean ± standard deviation. The results were obtained from 4–5 independent experiments using 20–24 wells. The statistical analyses were made using the Kruskal-Wallis test, followed by the Dunn's *post-hoc* test (*$p<0.05$ and ****$p<0.0001$ versus control; ####$p<0.0001$ versus PIX 0.1 μM; ++$p<0.01$, +++$p<0.001$ versus PIX 1 μM).
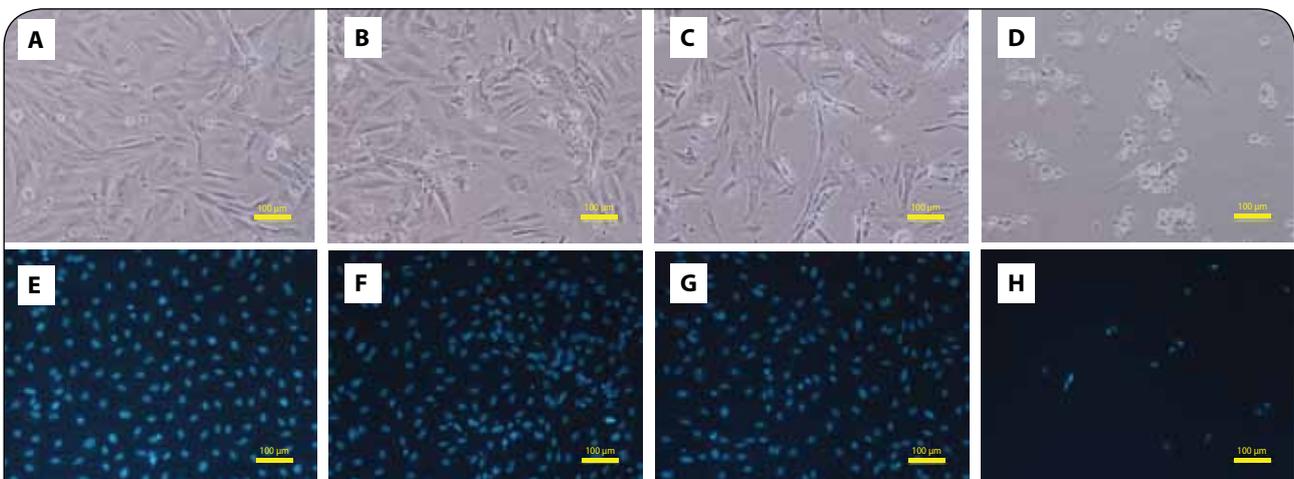
Figure 4. PIX evokes cellular damage in a concentration dependent manner in differentiated H9c2 cells. Phase contrast microscopy (A, B, C, D) and fluorescence microscopy (Hoechst 33258 staining) (E, F, G, H) images of 7-day differentiated H9c2 cells after a 48-h exposure to PBS (A and E), 0.1 μM PIX (B and F), 1 μM PIX (C and G) or 10 μM PIX (D and H). Images are representative of two independent experiments (scale bar 100 μm).
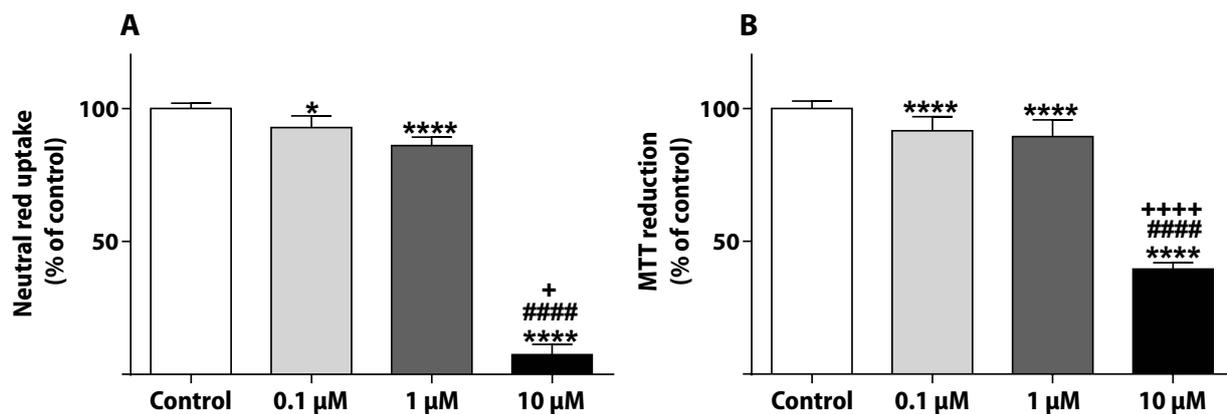
Figure 5. PIX induces lysosomal and mitochondrial disruption in differentiated H9c2 cells. NR uptake (A) and MTT reduction (B) assays in differentiated H9c2 cells exposed to 0.1, 1 or 10 μM PIX for 48 h. Values are expressed as percentage of control and are shown as mean ± standard deviation. The results were obtained from 4 independent experiments using 20 wells. The statistical analyses were made using the Kruskal-Wallis test, followed by Dunn's *post-hoc* test (A) and the ANOVA test, followed by the Tukey *post hoc* test (B) (*$p<0.05$ and ****$p<0.0001$ versus control; ####$p<0.0001$ versus PIX 0.1 μM; +$p<0.05$, ++++$p<0.0001$ versus PIX 1 μM).

ifosfamide, etoposide, MTX, or gemcitabine in a single agent therapy. The authors justified the higher frequency of cardiac adverse events in the PIX group by the presence of five patients within this group (compared with none in the comparator group) with previous histories of congestive heart failure or cardiomyopathy at the time of study enrolment (Pettengell *et al.,* 2012). However, two major issues, in our point of view, must be discussed that make PIX eligible as culprit of those cardiac events. More cardiac adverse events occurred in the PIX treatment group [24 of 68 (35.3%)] than in the comparator [14 of 67 (20.9%)], even when the comparator group had a higher median previous DOX dose equivalent of 315.5 mg/m^2 (range 15–681 mg/m^2), when compared to 292.9 mg/m^2 (range 51–472 mg/m^2) in the PIX group (Pettengell *et al.,* 2012). Moreover, patients in the comparator arm were treated with acknowledged cardiotoxic drugs (Pettengell *et al.,* 2012) but presented lower incidence of cardiotoxicity. In fact, FDA raised several issues regarding PIX cardiotoxicity, suggesting that PIX is indeed cardiotoxic, but gave no conclusions regarding the comparison of its toxicity to anthracyclines/anthracenediones (FDA, 2010). Our results support the idea that PIX is, in fact, cardiotoxic. In the morphological evaluation done through phase contrast microscopy, cellular damage was not evident following a 48-h exposure to 0.1 or 1 μM PIX, in non-differentiated H9c2 cells. Only at 10 μM PIX a significant damage was observed. Despite the clear reduction in the number of nuclei, especially seen in the highest PIX concentration tested (10 μM), in both differentiated and non-differentiated cells, no significant changes on nuclear morphology were evident when compared to control cells. These data indicate that PIX cytotoxicity may not elicit apoptosis in H9c2 cells in the time-point analyzed. Moreover, in the present work, two methods were used to evaluate the cytotoxicity of PIX, the MTT reduction and the NR uptake assays, which are extremely sensitive

in assessing cellular homeostasis impairment. The MTT colorimetric assay is based on mitochondrial activities of NADH dehydrogenase (complex I) and/or succinate dehydrogenase (complex II) on the tetrazolium salt with formazan formation (Costa *et al.,* 2009), whereas the NR uptake assay is based on the ability of viable cells to uptake the supravital dye that penetrates cell membranes and concentrates in lysosomes (Repetto *et al.,* 2008). Significant cytotoxicity was reported in both assays at all concentrations tested, being more pronounced for 10 μM PIX at 48 h, both in differentiated and non-differentiated H9c2 cells. The concentrations used here are clinically relevant, since 1 h after intravenous administration of doses ranging between 37.5 to 150 mg/m^2, the Cmax of PIX on the plasma of patients in a Phase I clinical trial was between 1–7 μM (Faivre *et al.,* 2001). The recommended dose of PIX is 50 mg/m^2 administered on days 1, 8, and 15 of each 28-day cycle for up to 6 cycles for the treatment of adult patients with multiple relapsed or refractory aggressive NHL (Péan *et al.,* 2013).

To the best of our knowledge, there is only one study with PIX in cardiac cellular models (Hasinoff *et al.,* 2016). For that reason, our results will be compared with the published data of other acknowledged cardiotoxic anticancer drugs, DOX and MTX, in *in vitro* models. Non-differentiated H9c2 cells exposed to 1 μM DOX at several time points (between 0 and 48 h) evidenced an increase in cell death with increasing time of exposure, evaluated through phase contrast microscopy (Zhang *et al.,* 2015). Regarding MTX, our group assessed the cytotoxicity of 5 μM and 2 μM MTX in differentiated H9c2 cells. After a 48-h exposure, an increase in cell death with increasing MTX concentrations was found (Reis-Mendes *et al.,* 2017). Based on these morphological data, PIX seems to cause lower damage when compared to DOX or MTX in the same cellular model, since only at the highest concentration tested (10 μM), a significant

damage was seen. Moreover, in our study with MTX, no signs of nuclear morphological alterations were observed after exposure to 2 or 5 µM MTX for 48 h in differentiated H9c2 cells (Reis-Mendes *et al.,* 2017), as evidenced here with PIX. However, in non-differentiated H9c2 cells, a 24-h exposure to 1.60 µM MTX or 0.9 µM DOX caused morphological signals of apoptosis (Kluza *et al.,* 2004) and caspase 3 activation occurred in non-differentiated H9c2 cells exposed for 24 h to 100 nM and 1 µM MTX (Rossato *et al.,* 2013).

In non-differentiated H9c2 cells, DOX elicited mitochondrial dysfunction as seen through the MTT reduction assay, following a 24-h exposure to 0.2, 1 and 5 µM (Zhang *et al.,* 2015). Regarding MTX, also in non-differentiated H9c2 cells, it led to a time- and concentration-dependent cytotoxicity (Rossato *et al.,* 2013). At 48 h, 10 µM MTX had values of around 20% when compared to control (100.0%) in the MTT assay, whereas 1 and 0.1 µM MTX showed values of approximately 80 and 90%, respectively, when compared to control cells (Rossato *et al.,* 2013). In the study carried out by our group using differentiated H9c2 cells exposed to various concentrations of MTX (0.01, 0.1, 1, 2 and 5 µM) for 48 h, 5 µM MTX showed values of around 75% in the MTT reduction assay, whereas 1 and 0.1 µM of 80% and 90%, respectively, when compared to control cells (Reis-Mendes *et al.,* 2017). The cytotoxicity caused by MTX is, in fact, very similar to what was observed in the present work with similar concentrations of PIX in non-differentiated and differentiated cells. Moreover, PIX, as did DOX, decreased the mitochondrial membrane potential of cardiac rat neonatal cardiomyocytes, thus demonstrating the ability of PIX to alter mitochondrial homeostasis (Hasinoff *et al.,* 2016) and its cardiotoxic potential.

Moreover, in the present work, 10 µM PIX caused a higher cytotoxicity in the NR assay in differentiated H9c2 cells when compared to non-differentiated cells. This assay also seems more sensitive to detect PIX cytotoxicity. On the other hand, using the same assay, differentiated H9c2 cells exposed for 48 h to 1 µM MTX incorporated 60% of NR when compared to control cells (set to 100%) (Reis-Mendes *et al.,* 2017), whereas with PIX, at the same incubation time and using the same concentration, the NR uptake was 76.25±8.21% in non-differentiated cells and 86.15±3.06% in differentiated cells. Additionally, 0.1 µM MTX did not cause any significant toxicity in the NR assay at 48 h in differentiated H9c2 cells (Reis-Mendes *et al.,* 2017), while 0.1 µM PIX decreased the dye's cellular incorporation to 87.07±6.09% in non-differentiated cells and to 93.51±3.22% in differentiated cells at the same incubation time point, further demonstrating the cardiotoxic potential of PIX. Most authors agree that using several cytotoxicity tests with different inherent mechanisms can help elucidate the underlying cytotoxicity of the drugs tested (Lopes *et al.,* 2008; Reis-Mendes *et al.,* 2017; Soares *et al.,* 2013).

The mechanisms involved in PIX putative cardiotoxicity are still undisclosed. In human leukemia K562 cells and contrasting with DOX, PIX produced no detectable semi-quinones or reactive oxygen species (ROS), possibly due to a lower PIX accumulation in those cells. The intracellular accumulation of PIX (1.5 nmol) was shown to be low when compared to MTX (8.1 nmol) or DOX (6.5 nmol) under the same experimental conditions (1 h incubation at 37 °C in a final concentration of 10 nmol) (Hasinoff *et al.,* 2016). Also, the spectrophotometric titrations of PIX suggested that, unlike what happens with DOX or MTX, PIX does not bind to Fe^{3+}, probably due to its lack of hydroquinone functionality (Herman *et al.,* 1997; Malisza and Hasinoff 1995). Fe^{3+} causes oxidative stress via the Fenton reaction and through formation of the highly toxic hydroxyl radical (Costa *et al.,* 2011). It is widely known that, in the heart, DOX forms a semi-quinone free radical and Fe^{3+}-DOX complexes, which are responsible for a futile redox cycle that creates oxidative stress (Costa *et al.,* 2013). MTX does not form ROS easily, but it affects the heart mitochondria (Reis-Mendes *et al.,* 2017; Rossato *et al.,* 2014; Rossato *et al.,* 2013), with the heart being largely susceptible to energetic dysfunction. According to Rossato *et al.,* the endpoint of toxicity induced by MTX is the electron transport chain and its dysfunction can create a mild oxidative stress that results in fatal cardiotoxicity (Rossato *et al.,* 2014; Rossato *et al.,* 2013). As stated before, PIX is able to decrease the mitochondrial membrane potential of cardiac rat neonatal cardiomyocytes (Hasinoff *et al.,* 2016) and mitochondria can be targets for PIX.

Additionally, compared to MTX and anthracyclines, PIX shows better selectivity for topoisomerase IIα (the form present in cancer cells) instead of IIβ (the form present in cardiomyocytes) at the 1–10 µM concentration range (Hasinoff *et al.,* 2016). The higher selectivity of PIX towards topoisomerase IIα led to the belief that PIX elicits low cardiotoxicity, since topoisomerase IIβ is the isoform present in cardiomyocytes and its inhibition can be responsible, at least partially, for the cardiotoxicity of DOX and MTX (Capranico *et al.,* 1992; Hasinoff *et al.,* 2016; Zhang *et al.,* 2012). However, the cardiac concentration of PIX after therapy is not known, and it may be sufficient to inhibit the physiological cardiac form of topoisomerase and thus cause cardiac dysfunction. In fact, cardiac dysfunction has been observed after PIX therapy, even if its use is not largely disseminated (Pettengell *et al.,* 2012; Volpetti *et al.,* 2014).

Overall, the two cytotoxicity assays performed in the present work show to be more sensitive to detect PIX-induced toxicity than Hoescht staining or phase contrast microscopy. In addition, differentiated H9c2 cells are slightly more prone to PIX induced cytotoxicity than non-differentiated H9c2 cells. Thus PIX toxicity is not dependent on its effects on cellular division, as the former model has a reduced proliferative state (Menard *et al.,* 1999; Reis-Mendes *et al.,* 2017). Despite the structural changes performed in the synthesis of PIX and its lower potential to form ROS and toxic drug metal complexes in human myocardial strip (Salvatorelli *et al.,* 2013), our work clearly shows its potential cardiac toxicity. This contradicts some of the data obtained in the scarce

clinical and preclinical studies done with PIX, where PIX is claimed as a cardiosafe drug when compared with its analogues (Beggiolin *et al.,* 2001; Borchmann *et al.,* 2003; Cavalletti *et al.,* 2007; Hasinoff *et al.,* 2016; Pettengell *et al.,* 2012). Actually, compared to the reports made for its predecessors, mainly with the works done in our group with MTX in the same cellular models (Reis-Mendes *et al.,* 2017; Rossato *et al.,* 2013), the data obtained here show that PIX has similar cardiac toxicity as MTX and should be regarded as a potential cardiotoxic drug.

Acknowledgments

REFERENCES

Beggiolin G, Crippa L, Menta E, Manzotti C, Cavalletti E, Pezzoni G, Torriani D, Randisi E, Cavagnoli R, Sala F, Giuliani FC, Spinelli S. (2001). Bbr 2778, an aza-anthracenedione endowed with preclinical anticancer activity and lack of delayed cardiotoxicity. *Tumori* **87**: 407–416.

Borchmann P, Morschhauser F, Parry A, Schnell R, Harousseau JL, Gisselbrecht C, Rudolph C, Wilhelm M, Gunther H, Pfreundschuh DM, Camboni G, Engert A. (2003). Phase-II study of the new aza-anthracenedione, BBR 2778, in patients with relapsed aggressive non-Hodgkin's lymphomas. *Haematologica* **88**: 888–894.

Capranico G, Tinelli S, Austin CA, Fisher ML, Zunino F. (1992). Different patterns of gene expression of topoisomerase II isoforms in differentiated tissues during murine development. *Biochim Biophys Acta* **1132**: 43–48.

Cavalletti E, Crippa L, Mainardi P, Oggioni N, Cavagnoli R, Bellini O, Sala F. (2007). Pixantrone (BBR 2778) has reduced cardiotoxic potential in mice pretreated with doxorubicin: comparative studies against doxorubicin and mitoxantrone. *Invest New Drugs* **25**: 187–195.

Conner CS. (1984). Mitoxantrone: a replacement for doxorubicin? *Drug Intell Clin Pharm* **18**: 479–480.

Corbett TH, Griswold DP Jr., Roberts BJ, Schabel FM Jr. (1981). Absence of delayed lethality in mice treated with aclacinomycin A. *Cancer Chemother Pharmacol* **6**: 161–168.

Costa VM, Carvalho F, Bastos ML, Carvalho RA, Carvalho M, Remião F. (2011). Contribution of catecholamine reactive intermediates and oxidative stress to the pathologic features of heart diseases. *Curr Med Chem* **18**: 2272–2314.

Costa VM, Carvalho F, Duarte JA, Bastos ML, Remiao F. (2013). The heart as a target for xenobiotic toxicity: the cardiac susceptibility to oxidative stress. *Chem Res Toxicol* **26**: 1285–1311.

Costa VM, Silva R, Tavares LC, Vitorino R, Amado F, Carvalho F, Bastos ML, Carvalho M, Carvalho RA, Remiao F. (2009). Adrenaline and reactive oxygen species elicit proteome and energetic metabolism modifications in freshly isolated rat cardiomyocytes. *Toxicology* **260**: 84–96.

Dawson LK, Jodrell DI, Bowman A, Rye R, Byrne B, Bernareggi A, Camboni G, Smyth JF. (2000). A clinical phase I and pharmacokinetic study of BBR 2778, a novel anthracenedione analogue, administered intravenously, 3 weekly. *Eur J Cancer* **36**: 2353–2359.

El-Helw LM, Hancock BW. (2007). Pixantrone: a novel aza-anthracenedione in the treatment of non-Hodgkin's lymphomas. *Expert Opin Investig Drugs* **16**: 1683–1691.

EMA. (2017). *Pixuvri (pixantrone): EU summary of product characteristics.* European Medicines Agency, London, UK.

Faivre S, Raymond E, Boige V, Gatineau M, Buthaut X, Rixe O, Bernareggi A, Camboni G, Armand JP. (2001). A phase I and pharmacokinetic study of the novel aza-anthracenedione compound BBR 2778 in patients with advanced solid malignancies. *Clin Cancer Res* **7**: 43–50.

FDA. (2010). *FDA ODAC Briefing Document: Pixuvri (pixantrone).* In: U.S.D.o.H.a.H. Services (Ed), Maryland, USA.

Hasinoff BB, Wu X, Patel D, Kanagasabai R, Karmahapatra S, Yalowich JC. (2016). Mechanisms of action and reduced cardiotoxicity of pixantrone; a topoisomerase II targeting agent with cellular selectivity for the topoisomerase II alpha isoform. *J Pharmacol Exp Ther* **356**: 397–409.

Herman EH, Zhang J, Hasinoff BB, Clark JR Jr., Ferrans VJ. (1997). Comparison of the structural changes induced by doxorubicin and mitoxantrone in the heart, kidney and intestine and characterization of the Fe(III)-mitoxantrone complex. *J Mol Cell Cardiol* **29**: 2415–2430.

Hescheler J, Meyer R, Plant S, Krautwurst D, Rosenthal W, Schultz G. (1991). Morphological, biochemical, and electrophysiological characterization of a clonal cell (H9c2) line from rat heart. *Circ Res* **69**: 1476–1486.

Hrynchak I, Sousa E, Pinto M, Costa VM. (2017). The importance of drug metabolites synthesis: the case-study of cardiotoxic anticancer drugs. *Drug Metab Rev* **49**: 158–196.

Kimes BW, Brandt BL. (1976). Properties of a clonal muscle cell line from rat heart. *Exp Cell Res* **98**: 367–381.

Kluza J, Marchetti P, Gallego MA, Lancel S, Fournier C, Loyens A, Beauvillain JC, Bailly C. (2004). Mitochondrial proliferation during apoptosis induced by anticancer agents: effects of doxorubicin and mitoxantrone on cancer and cardiac cells. *Oncogene* **23**: 7018–7030.

Krapcho AP, Petry ME, Getahun Z, Landi JJJr, Stallman J, Polsenberg JF, Gallagher CE, Maresch MJ, Hacker MP, Giuliani FC, Beggiolin G, Pezzoni G, Menta E, Manzotti C, Oliva A, Spinelli S, Tognella S. (1994). 6,9-Bis[(aminoalkyl) amino]benzo[g]isoquinoline-5,10-diones. A novel class of chromophore-modified antitumor anthracene-9,10-diones: synthesis and antitumor evaluations. *J Med Chem* **37**: 828–837.

Lopes MA, Meisel A, Dirnagl U, Carvalho FD, Bastos ML. (2008). Doxorubicin induces biphasic neurotoxicity to rat cortical neurons. *Neurotoxicology* **29**: 286–293.

Malisza KL, Hasinoff BB. (1995). Production of hydroxyl radical by iron(III)-anthraquinone complexes through self-reduction and through reductive activation by the xanthine oxidase/hypoxanthine system. *Arch Biochem Biophys* **321**: 51–60.

Menard C, Pupier S, Mornet D, Kitzmann M, Nargeot J, Lory P. (1999). Modulation of L-type calcium channel expression during retinoic acid-induced differentiation of H9c2 cardiac cells. *J Biol Chem* **274**: 29063–29070.

Péan E, Flores B, Hudson I, Sjöberg J, Dunder K, Salmonson T, Gisselbrecht C, Laane E, Pignatti F. (2013). The European Medicines Agency review of pixantrone for the treatment of adult patients with multiply relapsed or refractory aggressive non-hodgkin's b-cell lymphomas: Summary of the scientific assessment of the committee for medicinal products for human use. *Oncologist* **18**: 625–633.

Pettengell R, Coiffier B, Narayanan G, de Mendoza FH, Digumarti R, Gomez H, Zinzani PL, Schiller G, Rizzieri D, Boland G, Cernohous P, Wang L, Kuepfer C, Gorbatchevsky I, Singer JW. (2012). Pixantrone dimaleate versus other chemotherapeutic agents as a single-agent salvage treatment in patients with relapsed or refractory aggressive non-Hodgkin lymphoma: a phase 3, multicentre, open-label, randomised trial. *Lancet Oncol* **13**: 696–706.

Reis-Mendes A, Gomes AS, Carvalho RA, Carvalho F, Remiao F, Pinto M, Bastos ML, Sousa E, Costa VM. (2017). Naphthoquinoxaline metabolite of mitoxantrone is less cardiotoxic than the parent compound and it can be a more cardiosafe drug in anticancer therapy. *Arch Toxicol* **91**: 1871–1890.

Reis-Mendes AF, Sousa E, de Lourdes Bastos M, Costa VM. (2015). The role of the metabolism of anticancer drugs in their induced-cardiotoxicity. *Curr Drug Metab* **17**: 75–90.

Repetto G, del Peso A, Zurita JL. (2008). Neutral red uptake assay for the estimation of cell viability/cytotoxicity. *Nat Protoc* **3**: 1125–1131.

Rossato LG, Costa VM, Dallegrave E, Arbo M, Silva R, Ferreira R, Amado F, Dinis-Oliveira RJ, Duarte JA, de Lourdes Bastos M, Palmeira C, Remiao F. (2014). Mitochondrial cumulative damage induced by mitoxantrone: late onset cardiac energetic impairment. *Cardiovasc Toxicol* **14**: 30–40.

Rossato LG, Costa VM, Vilas-Boas V, de Lourdes Bastos M, Rolo A, Palmeira C, Remiao F. (2013). Therapeutic concentrations of mitoxantrone elicit energetic imbalance in H9c2 cells as an earlier event. *Cardiovasc Toxicol* **13**: 413–425.

Ruiz M, Courilleau D, Jullian JC, Fortin D, Ventura-Clapier R, Blondeau JP, Garnier A. (2012). A cardiac-specific robotized cellular assay identified families of human ligands as inducers of PGC-1alpha expression and mitochondrial biogenesis. *PLoS One* **7**: e46753.

Salvatorelli E, Menna P, Paz OG, Chello M, Covino E, Singer JW, Minotti G. (2013). The novel anthracenedione, pixantrone, lacks redox activity and inhibits doxorubicinol formation in human myocardium: insight to explain the cardiac safety of pixantrone in doxorubicin-treated patients. *J Pharmacol Exp Ther* **344**: 467–478.

Sardão VA, Oliveira PJ, Holy J, Oliveira CR, Wallace KB. (2009). Doxorubicin-induced mitochondrial dysfunction is secondary to nuclear p53 activation in H9c2 cardiomyoblasts. *Cancer Chemother Pharmacol* **64**: 811–827.

Soares AS, Costa VM, Diniz C, Fresco P. (2013). Potentiation of cytotoxicity of paclitaxel in combination with Cl-IB-MECA in human C32 metastatic melanoma cells: A new possible therapeutic strategy for melanoma. *Biomed Pharmacother* **67**: 777–789.

Stuart-Harris RC, Bozek T, Pavlidis NA, Smith IE. (1984). Mitoxantrone: an active new agent in the treatment of advanced breast cancer. *Cancer Chemother Pharmacol* **12**: 1–4.

Volpetti S, Zaja F, Fanin R. (2014). Pixantrone for the treatment of adult patients with relapsed or refractory aggressive non-Hodgkin B-cell lymphomas. *Onco Targets Ther* **7**: 865–872.

Zhang S, Liu X, Bawa-Khalfe T, Lu LS, Lyu YL, Liu LF, Yeh ET. (2012). Identification of the molecular basis of doxorubicin-induced cardiotoxicity. *Nat Med* **18**: 1639–1642.

Zhang YY, Meng C, Zhang XM, Yuan CH, Wen MD, Chen Z, Dong DC, Gao YH, Liu C, Zhang Z. (2015). Ophiopogonin D attenuates doxorubicin-induced autophagic cell death by relieving mitochondrial damage in vitro and in vivo. *J Pharmacol Exp Ther* **352**: 166–174.

Zordoky BN, El-Kadi AO. (2007). H9c2 cell line is a valuable in vitro model to study the drug metabolizing enzymes in the heart. *J Pharmacol Toxicol Methods* **56**: 317–322.